Analytica Chimica Acta 1027 (2018) 22–32

Contents lists available at ScienceDirect

Analytica Chimica Acta

journal homepage: www.elsevier.com/locate/aca

Highly-stable Li^+ ion-selective electrodes based on noble metal nanostructured layers as solid-contacts

Francesca Criscuolo*, Irene Taurino, Francesca Stradolini, Sandro Carrara, Giovanni De Micheli

Laboratory of Integrated System, EPFL, CH-1015, Lausanne, Switzerland

HIGHLIGHTS

- All-solid-state Li^+-ISEs with noble metal nanostructured layers as solid-contacts are developed.
- The gold and platinum nanostructures are prepared by a one-step electrodeposition procedure.
- The fabricated sensors offer Nernstian behavior, short response time and exceptional potential stability.
- High selectivity is achieved.

GRAPHICAL ABSTRACT

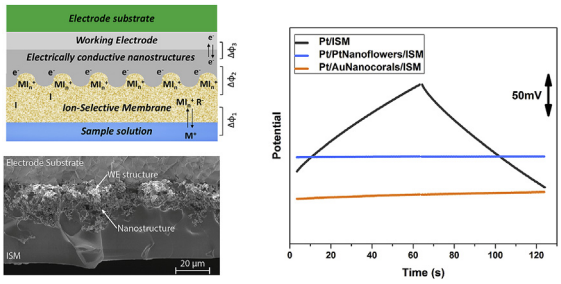

ARTICLE INFO

Article history:
Received 11 January 2018
Received in revised form
16 March 2018
Accepted 23 April 2018
Available online 11 May 2018

Keywords:
Solid-contact
All-solid-state ion-selective electrode
Potentiometry
Potential drift
Noble metal nanostructures
Lithium ions

ABSTRACT

Nowadays the development of stable and highly efficient Solid-Contact Ion-Selective Electrodes (SC-ISEs) attracts much attention in the research community because of the great expansion of portable analytical devices. In this work, we present highly stable Li^+ all-solid-state ISEs exploiting noble metals nanostructures as ion-to-electron transducers. The detection of lithium is essential for therapeutic drug monitoring of bipolar patients. In addition, greater environmental exposure to this ion is occurring due to the large diffusion of lithium-ion batteries. However, only a limited number of SC Li^+ ISEs already exists in literature based on Conductive Polymers (CPs) and carbon nanotubes. The use of noble metals for ion-to-electron transduction offers considerable advantages over CPs and carbon materials, including fast and conformal one-step deposition by electrochemical means, non-toxicity and high stability. We investigate for the first time the use of gold nanocorals obtained by means of a one-step electrodeposition process to improve sensor performance and we compare it to all-solid-state ISEs based on electrodeposited platinum nanoflowers. In addition, the effect of substrate electrode material, membrane thickness and conditioning concentration on the potentiometric response is carefully analysed. Scanning Electron Microscopy (SEM) and Current Reversal Chronopotentiometry (CRC) techniques are used to characterize the morphology and the electrochemical behaviour of the different ISEs. The use of nanostructured gold and platinum contacts allows the increase of the SC capacitance by one or two orders of magnitude, respectively, with respect to the flat metal, while the SC resistance is significantly reduced. We show that the microfabricated sensors offer Nernstian behaviour (58.7±0.8 mV/decade) in the activity range from 10^{-5} to 0.1 M, with short response time (~15 s) and small potential drift during CRC measurements ($\frac{dE}{dt} = 3 \times 10^{-5} \pm 2 \times 10^{-5}$ V/s). The exceptional response stability is verified also when no potential is applied. The sensor shows high selectivity towards all clinically important ions, with values very similar to conventional ISEs. Furthermore, to our knowledge, the selectivity towards Ca^{+2} is the best ever reported for SC-ISEs. In conclusion, the present study opens up new interesting perspectives

* Corresponding author.
E-mail address: francesca.criscuolo@epfl.ch (F. Criscuolo).

https://doi.org/10.1016/j.aca.2018.04.062

towards the development of simple and reproducible fabrication protocols to obtain high-quality and high-stability all-solid-state ISEs.

1. Introduction

Solid-Contact Ion-Selective Electrodes (SC-ISEs) have received considerable attention over the past 50 years towards next-generation portable and miniaturized ion-sensors with integrated steering circuits and read-out electronics [1]. Accurate and quantitative measurements of ions in solution are crucial in several different applications, including medical analysis [2,3], environmental [4] and water quality [5] monitoring, cosmetics [6], agriculture [7] and process control [8,9]. The first all solid-state ISE without internal reference solution was proposed in 1970 by Hirata and Date [10], followed by Cattrall et al. [11] the year after. Both systems were based on coated-wire electrodes. Poor reliability was achieved by Hirata and Catrall mainly because of the purely capacitive interface and the reduced contact area that caused large potential instabilities. Since then, several advances have been made thanks to the use of new SC materials and to better understanding of transport phenomena and water accumulation in the membrane. However, these systems still require major improvements since they suffer from some important limitations including the need of calibration, limited selectivity and potential drift. The most critical aspect is certainly represented by potential stability. There are mainly two possible causes of potential drift: the formation of a water layer at the ISM/SC interface and the small but non-zero current required for OCP measurements. In the first case, the sensor is generally sensitive to osmolality variations. Membrane delamination can eventually occur during operation because of poor adhesion to the substrate [1,12].

So far, the most promising candidates for commercial SC-ISEs are Conductive Polymers (CPs) and nanostructures with high double layer capacitance [13–15]. Nanostructured materials offer several advantages with respect to CPs, including the possibility to achieve high conductivity, the absence of possible side-reactions and the insensitivity to pH and light [1,16]. They exploit the electrical double layer that is formed at the membrane/electrode interface for ion-to-electron transduction: the accumulation of ions on one side of the interface thanks to the role of the ISM attracts electrons or holes on the other side; this leads to the formation of an asymmetric capacitor. In these systems the interfacial potential is not related to redox reactions, as in the case of CPs, or to ion partitioning, as in conventional ISEs, but to the amount of charge accumulated in the double layer. Thanks to their large surface area and their hydrophobic behaviour, nanostructured materials enable the achievement of good adhesion, avoiding the risk of water absorption. Moreover, they are typically characterized by high capacitance values. This property is crucial to reduce polarization effects due to the small but non-zero currents required for the measurement. For a more detailed description we refer the reader to [17]. Both carbon and noble metals nanostructures have been successfully investigated as SCs for ISEs: carbon nanotubes [18–21], fullerene [22,23], porous carbon [24–26], graphene [21,27–30], different polymer/carbon composites [31,32], platinum nanoparticles supported on carbon black [33], platinum nanopetals [34], gold nanodendrites [16], gold nanoclusters [35], nanoporous gold films [36] and gold nanoparticles [37,38]. An example of a SC-ISE based on MoO_2 microspheres has also been reported [39].

Many examples of portable SCs ion-sensors already exist in literature for most ions of clinical relevance. The research has focused mainly on cystic fibrosis and physical exercise monitoring. The most investigated ions are K^+ [23,34,37,40–48], Na^+ [45,49–52], Cl^- [47,53], NH^{4+} [48,54–56] and H^+ [48,52,57–59]. On the contrary, a very limited number of studies have been carried out in order to sense lithium ions.

Lithium salts represent the oldest yet effective drugs to treat psychiatric patients suffering of Bipolar Disorder (BD) in order to keep under control maniac episodes [60]. BD is a serious and potentially mortal disease, which cannot be cured, but only treated with specific drugs. It is characterized by episodes of depressed and maniac mood, separated by periods of normal mood. Maniac and depressed conditions can cause insomnia or hypersomnia, excessive weight loss/gain, suicidal thoughts, aboulia [61,62]. The risk of suicide is 30 times higher than in general population [63]. Consequently, after diagnosis, there is an urgent need of stabilization therapy [64]. Unfortunately, the therapeutic range of this compound is very narrow (0.5–1.5 mM) [65]. Moreover, dietary variations, interaction with other medicines as well as individual variability have a strong effect on the determination of the right dose [66]. The consequences of overdose can be extremely severe. They include drowsiness, ataxia, myoclonic twitching and chronic toxicity that can lead to irreversible damages to kidneys, liver and brain, and eventually to death [66]. Hence, Therapeutic Drug Monitoring (TDM) is crucial to optimize the dose for each patient [67]. More specifically, lithium concentration in serum must be controlled at least every week (standardized 12h or 24h Li^+ serum concentration) at the beginning of the treatment or after any change in the dose. The time interval between subsequent check-ups can be enlarged only in absence of any complications. On the contrary, the frequency of serum lithium analyses should be increased accordingly. Check-ups every three month must be performed during maintenance [60].

Lithium quantification in clinical laboratories is routinely performed by atomic absorption spectrometry, flame emission photometry or conventional ISEs [68]. The possibility to use colorimetry [65] and photometry [69,70] has also been reported in literature [68]. Obviously, all these techniques require highly qualified personnel and expensive equipment. In this regard, all-solid-state SC-ISEs constitute ideal candidates for the development of low-cost and easy-to-use sensors for decentralized monitoring of lithium that would avoid frequent check-ups in hospital to the patients. Novell et al. have reported the fabrication of a paper-based Li^+ ion-selective sensor using carbon nanotubes as SCs [71]. Coldur et al. have fabricated a miniaturized Li^+ ISE with improved selectivity using a graphite composite to achieve ion-to-electron transduction [72]. In the following years they have also reported the determination of lithium under flowing conditions towards the development of automatic and LOC analytical devices [73]. All these sensing systems open up new interesting perspectives, but some limitations must still be tackled, including biocompatibility and toxicity, reproducibility and simplicity of the fabrication process.

Other possible applications of lithium sensors may also arise from the expanding use of lithium-ion batteries that is likely to bring greater environmental exposure through leaching of landfill [74].

In this paper, we present highly stable Li^+ ISEs based on noble

metals nanostructured SCs. These materials offer several advantages over carbon materials and conductive polymers, including fast and conformal one-step electrodeposition, high stability, non toxicity and increased surface area. SCs based on gold nanocorals are employed for the first time and compared to platinum nanoflowers to overcome the pervasive challenge of potential drift in current ISEs technology. In all cases, a one-step electrodeposition procedure is used, allowing a much simpler and faster fabrication protocol with respect to the previously reported gold nanoporous SCs [36]. In addition, the effect of different substrates and conditioning protocols is deeply investigated. The various ISEs are characterized morphologically and electrochemically by Scanning Electron Microscopy (SEM) and Current Reversal Chronopotentiometry (CRC) measurements. It is found that the use of nanostructured gold and platinum contacts allows the increase of the SC capacitance by one or two orders of magnitude, respectively, with respect to the flat metal, while the SC resistance is significantly reduced. The microfabricated sensors offer Nernstian behaviour with short response time (~15 s) and small potential drift during CRC measurements ($\frac{dE}{dt} = 3 \times 10^{-5} \pm 2 \times 10^{-5}$ V/s). The exceptional stability of sensor response is also verified when no potential is applied. Low Limit Of Detection (LOD) and high selectivities are obtained, with values comparable to the ones reported for conventional ISEs. To our knowledge, we achieve the highest selectivities towards Ca^{2+} ever reported for SC-ISEs. In conclusion, the proposed technology represents a simple and reproducible fabrication method that can be applied to obtain high-quality and high-stability all-solid-state ISEs for different applications.

2. Experimental methods

2.1. Materials

Platinum and gold Screen Printed Electrodes (SPEs) with an active area of 12.56 mm^2 were purchased from Metrohm (Switzerland). All chemicals were purchased from Merck (Germany).

2.2. ISM fabrication

After the electrochemical cleaning of the electrodes [34], noble metals nanostructures were electrodeposited onto platinum and gold screen printed electrodes using an Autolab Potentiostat controlled by Nova Software (Metrohm, Switzerland). Gold and platinum nanostructures were deposited by applying a potential of −3 V in $HAuCl_4$ 5 mM, NH_4Cl 1.25 M for 120 s and −1 V in 50 mM H_2SO_4, 25 mM H_2PtCl_6 for 200 s, respectively, using a three-electrodes setup. A K0265 Ag/AgCl Reference Electrode from Ametek (United States) was used for all depositions. A volume of 10 µl of membrane cocktails consisting of 28.00 wt% Poly (vinyl chloride) high molecular weight, 1 wt% Li Ionophore VI (6,6-Dibenzyl-1,4,8-11-tetraoxacyclotetradecane), 0.7 wt%, Potassium tetrakis (4-chlorophenyl)borate and 70.3 wt% 2-Nitrophenyl octyl ether for 100 mg of mixture dissolved in 1 mL of Tethraydrofuran (THF) was drop-casted on SPEs. The membrane was kept at dark for 24 h to allow solvent evaporation. Subsequently, the ISE was conditioned for 24 h at 0.01 M LiCl, unless otherwise stated.

2.3. Morphological characterization

Scanning Electron Microscopy was used for the morphological characterization of the electrodes. No sample pre-treatments were performed. The SEM analysis was carried out at the Interdisciplinary Centre of Electronic Microscopy (CIME) of École Polytechnique Fédérale de Lausanne (EPFL) by using a Merlin microscope from Zeiss (resolution up to 0.6 nm in STEM mode, probe current up to 300 nA, acceleration voltage 20 V to 30 kV) in SE mode. The accelerating voltage used for the SEM imaging is in the range 2–5 kV. The images of the nanostructured SCs were taken with an *In-Lens* detector at a Working Distance (WD) of 6 mm, while all others with an *HE-SE2* detector at a WD of 2.7 mm. The analysis of the different ISM thicknesses for different solution volumes was performed with a Xlf-30 scanning electron microscope at CIME (resolution up to 2 nm at 30 kV and 8 nm at 1 kV, acceleration voltage 1 kV–30 kV) in SE mode. The electrodes have been broken to visualize their cross sections and to measure the average height of the deposited membrane, as in Fig. 1b. An accelerating voltage of 2 kV and a WD of 9.4 mm were set for these measurements.

2.4. Electrochemical measurements

All potentiometric measurements were performed in a two-electrodes cell setup by means of an Autolab potentiostat with Nova Software (Metrohm, Switzerland). A double junction Sension+ 5044 Reference Electrode (Hach, United States) for use with ISE was employed in all potentiometric measurements.

Cyclic Voltammetric measurements were performed in a three-electrodes configuration using a K0265 Ag/AgCl Reference Electrode from Ametek (United States). A 5 mM ferro/ferricyanide aqueous solution was employed.

3. Experimental results and discussion

A scheme of the ISEs with noble metal nanostructured SCs that have been used in this work is given in Fig. 1. Both gold and platinum nanostructured layers were developed previously to achieve sensitive detection of glucose [34,75]. The platinum nanoflowers were also investigated to build a K^+ ISM on a platinum electrode

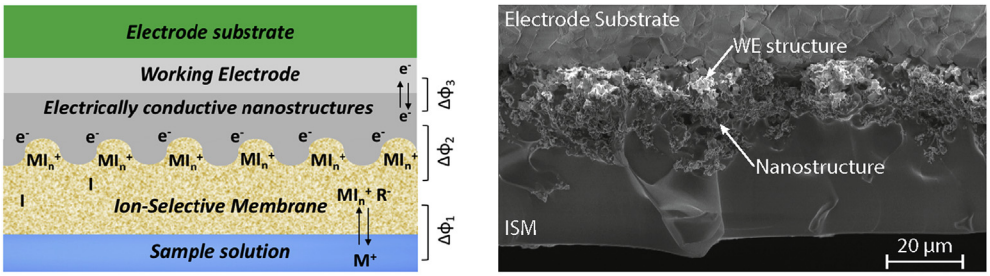

(a) (b)

Fig. 1. a) Scheme of the fabricated nanostructures-based SC-ISEs. b) SEM cross-sectional view of a Li^+ ISE with platinum nanoflowers as SC.

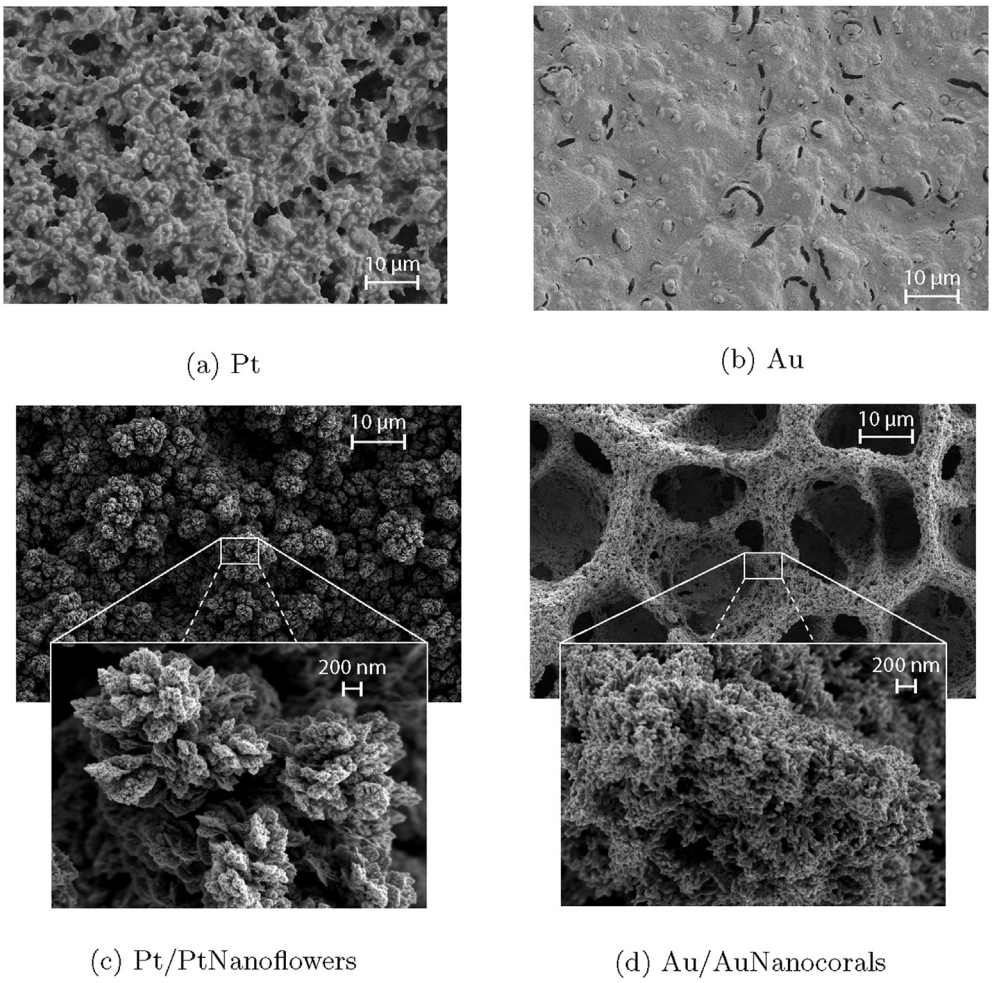

Fig. 2. SEM images of Pt/PtNanoflowers and Au/AuNanocorals SCs at different fabrication steps for: bare electrodes (a–b); electrodes after nanostructuring (c–d).

microfabricated by standard lithographic methods and metal evaporation. In this work, for the first time, we use and compare these nanostructures to fabricate Li^+ ISM with improved sensing performance. We employ SPEs instead of the evaporated ones used in Ref. [34]. Both gold and platinum substrates are investigated as electrode materials.

3.1. Morphological characterization

SEM images were taken at different fabrication steps. In particular, the morphology of gold and platinum SPEs was investigated before and after the electrochemical nanostructuration of the substrate material. The bare platinum and gold SPEs are depicted in Fig. 2a and b, respectively. SEM images of platinum nanoflowers deposited on a platinum SPE are shown in Fig. 2c, while gold nanostructures on a gold SPE are reported in Fig. 2b. It is evident that in all cases conformal and homogeneous depositions are obtained, despite the active area of the SPEs is larger than the microfabricated electrodes used in Ref. [34]. The platinum nanostructures form a highly branched fractal architecture. On the contrary, the electrochemically deposited gold is organized in pores with dimensions in the order of tens of micrometers. These are made of nanocoral-shaped features, as evident from the pictures at higher magnifications (zoom in Fig. 2c and d). In general, it is possible to conclude that the electrochemical deposition of platinum and gold nanostructures allows the shift from micro-to nanoscale surface roughness, thus allowing significant increase in the surface area of the electrode. Cross depositions of platinum nanoflowers on gold substrates and of gold nanocorals on platinum ones were also performed. No significant effect of substrate material on surface morphology was found, therefore we are not reporting the images here.

The Supplementary Material includes the SEM pictures of the ISM membranes before and after the electrochemical measurements on Pt/PtNanoflowers (Fig. S1) and Au/AuNanocorals (Fig. S2) SCs. No significant difference in topography was found after ISEs usage.

3.2. Characterization by Current Reversal Chronopotentiometry (CRC) and Cyclic Voltammetry (CV)

The electrochemical performance of Li^+ ISEs with and without nanostructured SCs on different substrates were compared by means of CRC measurements. This is a useful method to investigate potential stability. A direct current of a few nA is applied for certain time and then reversed, while measuring the sensor potential. The E-t curves show two main features: a jump when the change in current direction occurs and a slow potential drift at longer times [76].

The CRC measurements with and without nanostructured SCs on platinum and gold SPEs are given in Figure 3a and 3b, respectively. It is evident that in both cases the presence of

nanostructured SCs radically improves potential stability with respect to the ISM directly deposited on the platinum and gold SPEs. This phenomenon can be attributed to the different ion-to-electron transduction mechanism that is exploited by nanostructured materials [1] (Fig. 1a): the ISM traps the target ions; consequently, an accumulation of electrons is induced on the other side of the ISM and an asymmetric capacitor is formed. The interfacial potential is not related to redox reactions, as in the case of SCs based on CPs, or to ion partitioning, as in conventional ISEs, but to the amount of charge accumulated in the double layer. Nanostructured-based SCs have typically high capacitance values. This property greatly reduces the risk of polarization effects due to the small but non-zero currents required for the measurement. In addition, improvement in membrane adhesion is in general achieved thanks to the large surface area. This property is important to minimize the risk of water absorption, that will cause high sensitivity to osmolality variations and structural damages of the membrane, eventually leading to the mechanical failure by delamination.

All four combinations of nanostructures-substrates were investigated and compared. The CRC responses of platinum and gold nanostructures are shown in Fig. 4a for platinum substrates and in Fig. 4b for gold electrodes. The curves of three different samples for each stack sequence are reported to compare reproducibility. It is possible to observe that platinum nanoflowers SCs seem to offer a slightly more stable response with respect to gold nanocorals. In addition, the response of different sensors with the same stack spans in a much narrower potential range for platinum nanoflowers than for gold nanocorals. This is observed on both gold and platinum substrates. This property is important towards the development of calibration-free sensors, that is still one of the major concerns in current SC-ISEs technology.

In order to obtain quantitative comparison among different samples to corroborate previous discussion, the resistance, potential drift and capacitance values of the different SC-ISEs were computed from the CRC results. Their values are reported in Table 1. Five samples for each stack sequence were considered. The total resistance of the electrode can be determined from the potential jump simply using Ohms law (V = Ri). From the table, it is possible to see that the use of noble metal nanostructures significantly decreases the contact resistance both on gold and platinum substrates, thus enhancing charge transfer at the SC interface. In particular, a reduction of one order of magnitude is obtained with nanostructured SC. Platinum nanoflowers allow the largest improvement in SC conductivity. The lowest resistance value is achieved when Pt/PtNanoflowers SCs are used. As expected the bare gold electrodes have a lower contact resistance with respect to the platinum ones since this metal is characterized by higher electrical conductivity. The potential drift is defined by the slope of the curve [12,77]. The use of gold and platinum nanostructured SCs allows a slope reduction of one and two orders of magnitudes, respectively, with respect to ISMs directly deposited on the SPEs. In particular, when using platinum substrates, the potential drift decreases from 1.80±0.29 mV/s without nanostructured SCs down to 0.12±0.06 mV/s with gold nanocorals and 0.03±0.02 mV/s with platinum nanoflowers. The capacitance values of the SC can be deducted according to the following equation: $C = \frac{i}{dE/dt}$, where i is the applied current [1]. The highest SC capacitance is achieved by depositing platinum nanoflowers (195.3±96.8 μF) on platinum electrodes. Gold nanocorals have a capacitance in the range of several tens of μF, which is still one order of magnitude larger than the bare SPEs. This value is comparable or slightly higher with respect to the one reported for the electrodeposited nanoporous gold in Ref. [36]. However, the main advantage of our approach is the fast one-step electrodeposition procedure adopted for electrode nanostructuration.

The significant increase in electrode capacitance with nanostructured SCs was corroborated also by Cyclic Voltammetry (CV). The CV measurements were performed in an aqueous solution containing the ferro/ferricyanide redox couple. From Fig. 5, it is

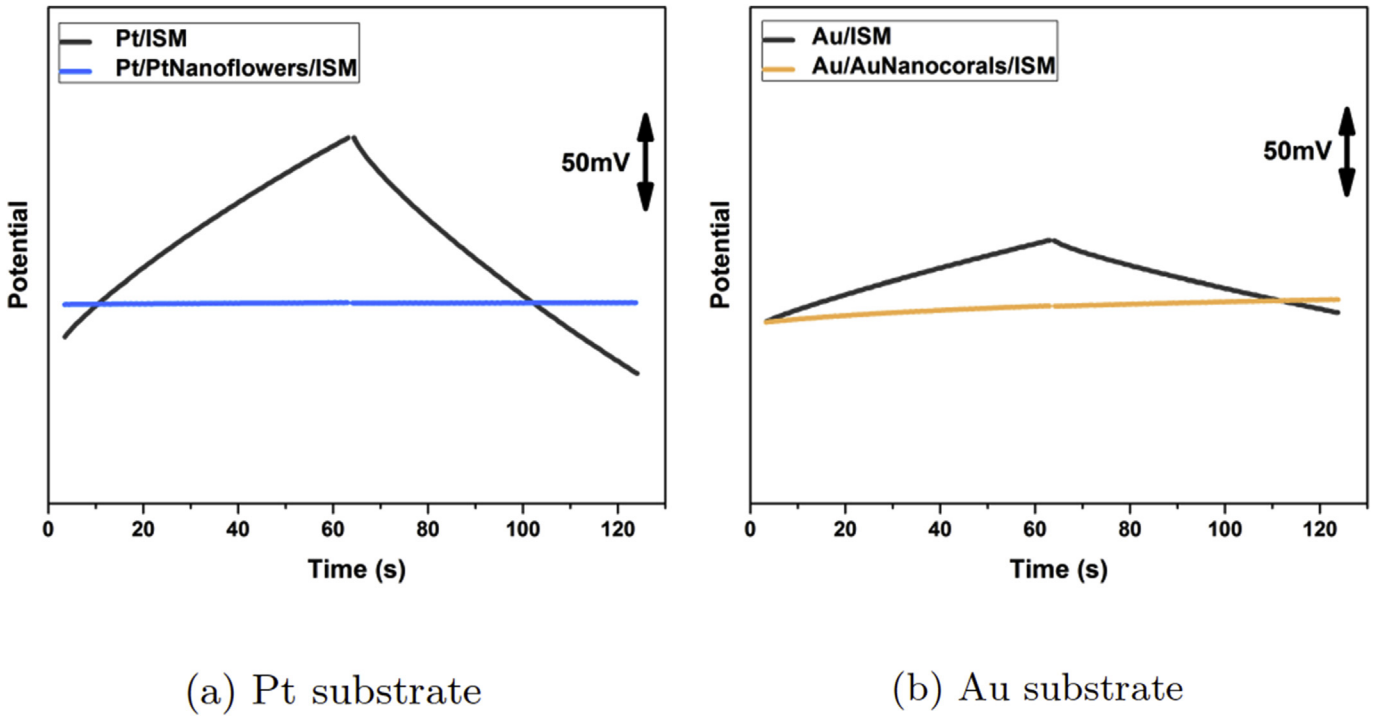

Fig. 3. CRC measurements of all-solid-state Li^+ ISEs on platinum (a) and gold (b) substrates showing the significant improvement in potential stability when nanostructured SCs are used. (±5 nA for 60 s in 0.01 M LiCl solution).

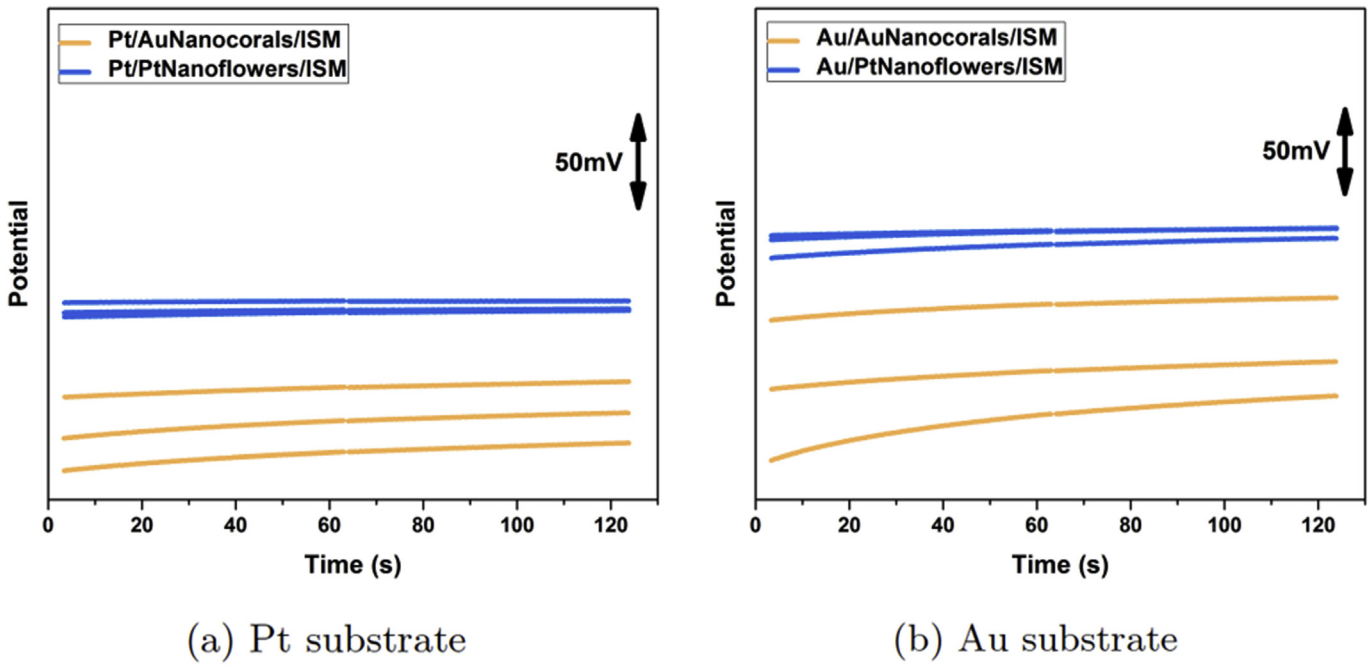

Fig. 4. CRC comparison of different stacks of nanostructured Li^+ SC-ISEs. In particular, gold nanocorals and platinum nanoflowers were employed as SCs on both platinum (a) and gold (b) substrates. (±5 nA for 60 s in 0.01 M LiCl solution).

Table 1
The total resistance, potential drift and capacitance values of the different fabricated Li^+ ISEs have been computed from the CRC measurements. Five samples for each stack sequence were fabricated and tested.

	R [kΩ]	dE/dt [mV/s]	C [μF]
Pt/ISM	146±76	1.80±0.29	2.5±0.1
Pt/PtNanoflowers/ISM	28±4	0.03±0.02	195.3±96.8
Pt/AuNanocorals/ISM	41±19	0.12±0.06	50.5±24.0
Au/ISM	108±54	0.76±0.43	9.5±6.7
Au/PtNanoflowers/ISM	51±11	0.07±0.05	113.7±96.9
Au/AuNanocorlas/ISM	30±21	0.21±0.14	29.4±13.7

possible to see that the use of nanostructured SCs greatly improves the capacitive current of the system. In particular the highest capacity is achieved with platinum nanoflowers SCs, as found in the CRC measurements. In addition, the better CRC performance achieved on platinum substrates was also confirmed, as evident from the larger integral area of the voltammograms with respect to ISM on gold substrates.

In conclusion, the CV measurements and the resistance and capacitance values calculated from CRC confirm the improved stability of the nanostructured SC produced in this work that was evident from a first qualitative analysis of CRC graphs in Fig. 4. Platinum nanoflowers seem to offer a slightly better performance than gold nanostructures in terms of potential stability and reproducibility, thus they will be the SC of choice in the following discussion, unless otherwise stated. By comparing the capacitance values of the different ISMs on the two substrates, it is also possible to state that in all cases platinum SPEs show a slightly higher capacitance with respect to the gold ones. Consequently, this substrate will be in general preferred in subsequent argumentation. The Pt/PtNanoflowers SC used in this work shows a much higher capacitance value with respect to the all-solid-state ISEs based on other commonly used nanostructures, including carbon nanotubes [18], graphene [27,29], reduced graphene oxides [30], graphene-polymer composites [31], fullerenes [22], but also of MoO_2 microspheres [39], platinum nanoparticles [33], gold nanodendrites [16] and nanoporous gold [36]. In addition its value is comparable to the capacitance of the SCs based on gold nanoclusters reported in Ref. [35]. Only [26] and [32] show higher capacitance values using porous carbon and carbon-black SCs, respectively.

3.3. Sensor calibration

The beneficial effect of electrode nanostructuring is also evident from the calibration time traces in Fig. 6. Non-nanostructured electrodes (black and grey curves) show large potential instabilities and significant background signal. On the contrary, the ISE based on platinum nanoflowers offer a very smooth response (blue curve). Sharp steps are generated by successive increments in lithium concentration. In addition, a small increase in the background signal with time occurs in the presence of nanostructured SCs.

An example of a typical calibration curve computed from the potentiometric time trace is given in Fig. 7 for an ISE with platinum nanoflowers as SC on a platinum SPE. A summary of all sensor parameters are reported in Table 2. The sensor shows a near-Nernstian behaviour with a slope of 58.7±0.8 mV/decade. It is important to notice that also the standard deviation is decreased by a factor of two with respect to the literature value, thus corroborating the good reproducibility of the system that was evident also from the CRC results. The limit of detection was computed according to IUPAC definition as the intersection of the linear portions of the curve [77]. Its value was found to be around 1.3×10^{-5} M. Although higher than in other papers [72], it is still satisfactory because well below the minimum effective concentration of the lithium drug (0.5 mM [65]). In addition, the response time of the sensor is always very short, as evident from the sharp steps in the calibration time trace of Fig. 6.

3.4. Effect of conditioning concentration and membrane thickness

The effect of conditioning concentration on the sensor was also investigated. Fig. 8a shows the calibration curves between 10^{-7} M

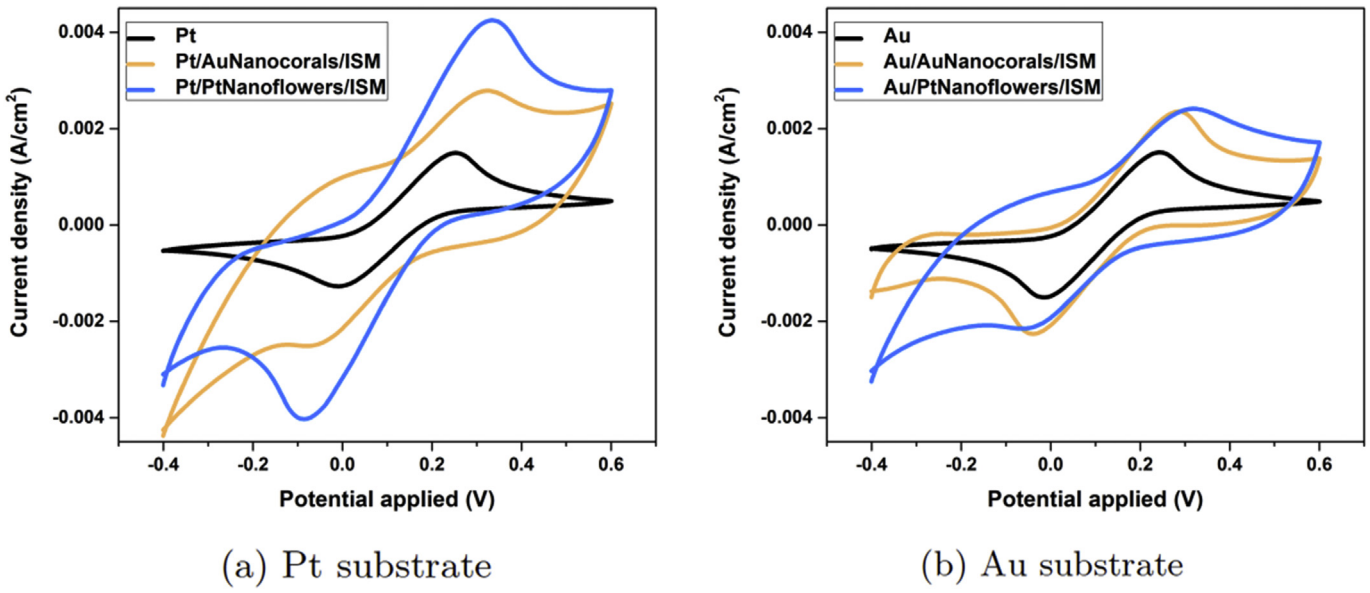

Fig. 5. Cyclic voltammograms in a 5 mM potassium ferro/ferricyanide solution of: a) Pt, Pt/PtNanoflowers and Pt/AuNanocorals SCs; b) Au, Au/PtNanoflowers and Au/AuNanocorals SCs. It is evident that electrode nanostructuring significantly increases the SC capacitance, as expected. (scan rate 100 mV/s).

and 0.1 M after conditioning at different concentrations for 24 h. It is possible to conclude that lower concentrations bring the membrane to higher potential ranges, on the contrary to what could be expected. No significant effect on the LOD was found. However, if we repeat the calibration in a narrow concentration range close to the therapeutic window values, the conditioning concentration is found to have a major role in sensor response, as evident from Fig. 8b. In particular, it is possible to conclude that the 0.01 M LiCl solution improves the linearity of the system and greatly reduces standard deviation, providing improved prediction accuracy. This will be the conditioning concentration of choice in following discussion.

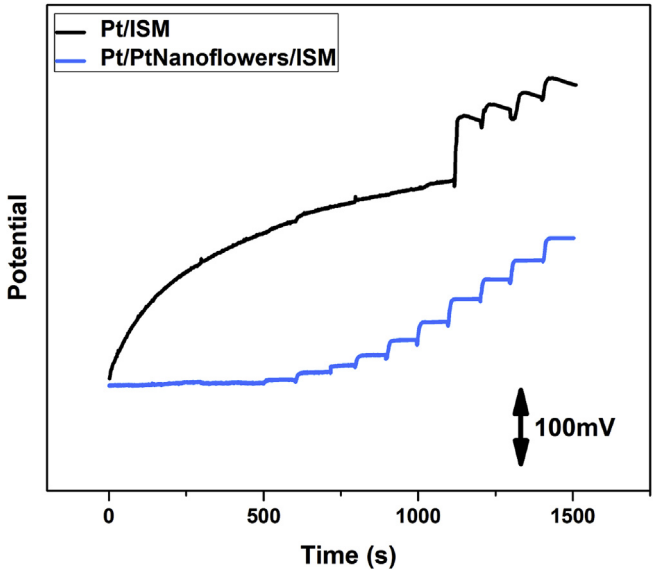

Fig. 6. Example of potentiometric time traces obtained during the calibration of Li^+ SC-ISEs with (blue curve) and without (black curve) nanostructured SC. The use of platinum nanoflowers allows the achievement of a much more stable potential response. (For interpretation of the references to color in this figure legend, the reader is referred to the Web version of this article.)

The ISM thickness was varied by increasing the cocktail volume drop-casted on the electrode. As expected the increase in drop-casted solution leads to the formation of thicker membrane until a maximum value is reached (reported in the Supplementary Material, Fig. S3). Above this saturation value the excess solution simply spreads around the electrode. The influence of ISM

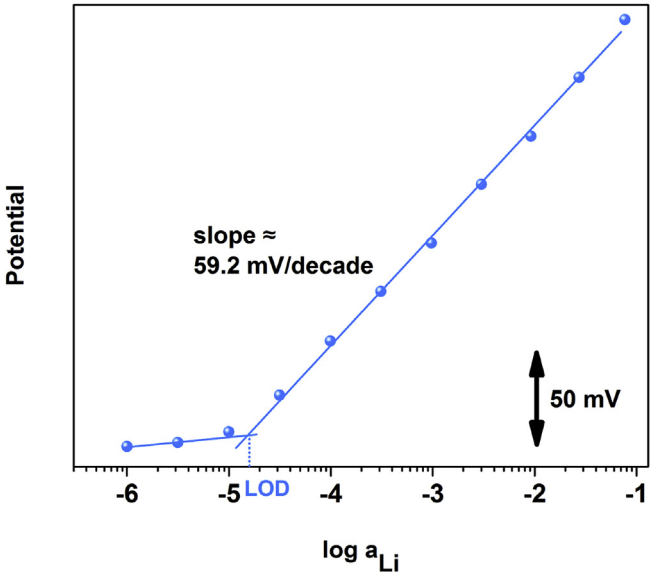

Fig. 7. Example of a typical calibration curve of Li^+ ISEs with platinum nanoflowers as SCs.

Table 2
Analytical parameters of Li^+ SC-ISEs based on Pt/PtNanoflowers SCs.

	This work	Literature
sensitivity [mV/decade]	58.7±0.8	59.8±1.4 [71]
LOD [M]	$13 \times 10^{-6} \pm 4 \times 10^{-6}$	5×10^{-6} [72]
Response time [s]	15–30	20 [72]
pH stability	from 4 to 12	from 4 to 12 [71]

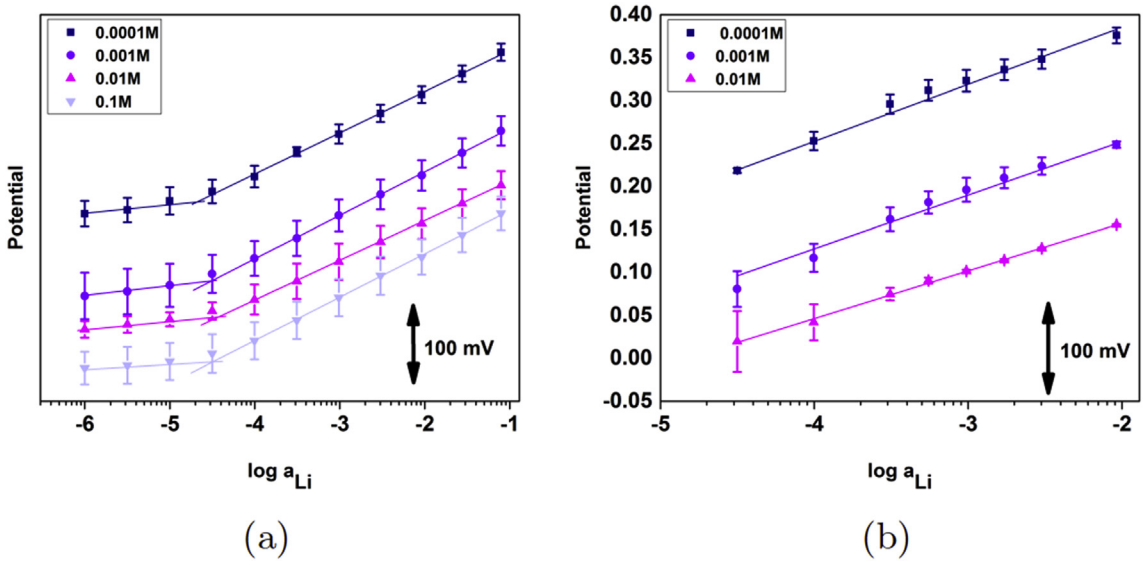

Fig. 8. Calibration curves of Li^+ ISEs based on platinum nanostructured SCs after conditioning at different concentrations: a) long range calibration range (between 10^{-6} M and 0.1 M); b) short range calibration around the therapeutic window values.

thickness on sensor performance was investigated. However, no significant effect of membrane thickness on Nernstian behaviour, LOD and selectivity was found. In general a solution volume of 10 μl was drop-casted in this work, unless otherwise stated, in order to allow complete coverage of the electrode while limiting chemical consumption.

3.5. Stability of potential response

The predictability of the sensor signal was investigated by comparing the potential developed by the system when exposed to a 0.01 M LiCl solution with the previously obtained calibration curve. The percentage difference between the potential value predicted from the calibration curve and the one measured in a constant concentration solution was found to be very small (0.58±0.46%). A reversed sensor calibration was also performed in the range 10^{-5} M and 0.1 M (Fig. 9a). The curve corroborates previous results, proving the good stability and reversibility of the sensor response. In addition, potential drift over time was found to be very limited in the concentration range of interest, as evident from Fig. 9b, that shows the trend of the potential value over time of two fabricated sensors when placed in a 1 mM LiCl solution for a long period of time.

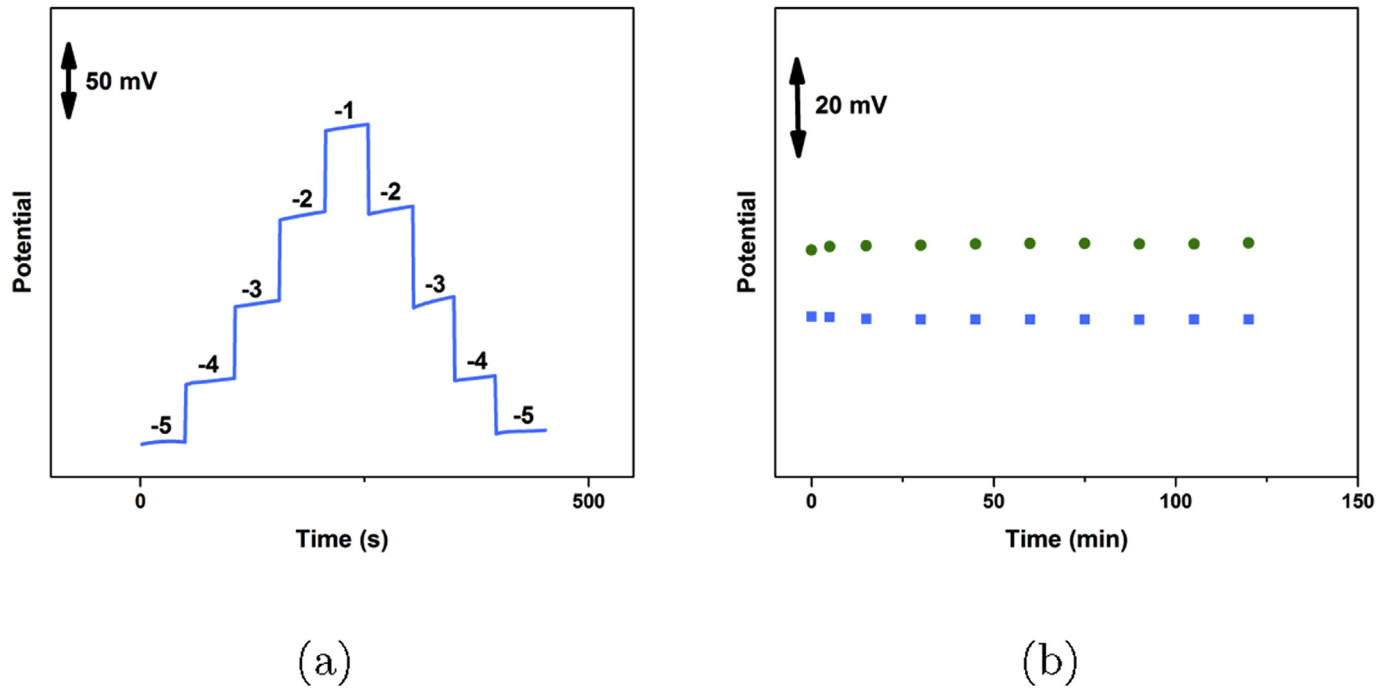

Fig. 9. a) Reversed calibration of Li^+ ISEs based on platinum nanostructured SCs between 10^{-5} M and 10^{-1} M (the logarithm of the concentration is reported above the corresponding potential step. b) Potential stability over time of two Li^+ ISEs based on platinum nanostructured SCs during immersion in a 3 mM LiCl solution.

Table 3
Selectivity coefficient of Li^+ ISEs based on platinum nanostructured SCs for different interfering ions obtained by SSM and FIM in comparison with the highest literature values.

	Log $K_{Li^+,int}$			
	K^+	Na^+	NH^{4+}	Ca^{2+}
SSM	−2.38±0.25	−2.67±0.23	−2.97±0.21	−3.90±0.08
FIM	−2.56±0.12	−2.55±0.17	−3.08±0.16	−4.01±0.05
Literature (SSM)	−3.34 [71]	−3.11 [71]	−3.29 [71]	−3.36 [79]
Conventional ISE (FIM)	−2.3 [80]	−2.5 [80]	−3.1 [80]	−4.3 [80]

3.6. Selectivity studies

The selectivity of the sensor was investigated by comparing different methods. The values obtained by the Separate Solution Method (SSM) and the Fixed Interference Method (FIM) are reported in Table 3 in comparison with the highest values reported in literature both for conventional and all-solid-state Li^+ ISEs. For the SSM the procedure described in Ref. [78] was used to achieve unbiased selectivity values. Entire calibration curves were taken for each ion to determine their Nernstian range. In the FIM a fixed interfering ion activity of 2.8×10^{-2} was used during all sensor calibrations. To our knowledge, no FIM values for Li^+ SC-ISEs have been reported in literature yet.

The here presented Li^+ ISEs show the highest selectivity towards Ca^{2+} ever obtained for SC-ISEs. As expected the lowest selectivity coefficients are the ones for the smallest ions, K^+ and Na^+, since they have similar dimensions to Li^+ ions, thus giving larger interference. In particular, selectivity values of about 1:450 and 1:180 are achieved in this work for K^+ and Na^+, respectively. Although lower, than in other works [71], this performance is still acceptable. The selectivity versus NH^{4+} ions is very similar to the highest value reported in literature. In conclusions, all selectivity values are very similar to the ones reported for conventional ISEs.

4. Conclusions

In this paper, we have developed all-solid-state Li^+ ISEs exploiting noble metals nanostructures as ion-to-electron transducers. In particular, gold nanocorals deposited in a fast and conformal one-step electrochemical deposition process are used for the first time as SCs and compared with similarly obtained platinum nanoflowers. Conformal deposition and improved surface area were demonstrated by means of SEM. The nanostructures performance on different substrate electrode materials and the influence of the conditioning procedures were deeply investigated. Electrochemical measurements proved the reduced charge transfer resistance, large capacitance, exceptional potential stability and excellent analytical performance of the sensors. All selectivity values are found to be very close to the ones reported for conventional ISEs. In addition, the highest selectivity towards Ca^{2+} ever obtained for Li^+ SC-ISEs is achieved. In conclusion, the fabrication method presented in this work can be considered as an important step towards the development of portable systems for monitoring of lithium ions since a very limited number of research works have been carried out in this regard. The nanostructured SCs proposed in this paper offer several advantages, including fast deposition, high stability and non-toxicity, thus they can be employed to obtain high-quality and high-stability all-solid-state ISEs for other target ions in different fields of applications.

Conflicts of interest

There are no conflicts to declare.

Acknowledgements

This research is supported by H2020 ERC 2014 ADG669354 CyberCare. The author would like to thank Dr. Nadezda Pankratova for the fruitful discussions on potentiometric sensing and selectivity calculations.

Appendix A. Supplementary data

Supplementary data related to this article can be found at https://doi.org/10.1016/j.aca.2018.04.062.

References

[1] J. Hu, A. Stein, P. Bühlmann, Rational design of all-solid-state ion-selective electrodes and reference electrodes, Trends Anal. Chem. 76 (2016) 102–114, https://doi.org/10.1016/j.trac.2015.11.004. https://doi.org/10.1016/j.trac.2015.11.004.
[2] A. Lewenstam, Routines and challenges in clinical application of electrochemical ion-sensors, Electroanalysis 26 (6) (2014) 1171–1181, https://doi.org/10.1002/elan.201400061.
[3] G. Matzeu, L. Florea, D. Diamond, Advances in wearable chemical sensor design for monitoring biological fluids, Sens, Actuators B 211 (2015) 403–418, https://doi.org/10.1016/j.snb.2015.01.077. https://doi.org/10.1016/j.snb.2015.01.077.
[4] G. Matzeu, C. Zuliani, D. Diamond, Recent progress in disposable ion-selective sensors for environmental applications, Adv. Sci. Technol. 77 (2012) 65–70, https://doi.org/10.4028/www.scientific.net/AST.77.65. http://www.scientific.net/AST.77.65.
[5] W.Y. Chung, J.H. Yoo, Remote water quality monitoring in wide area, Sens, Actuators B 217 (2015) 51–57, https://doi.org/10.1016/j.snb.2015.01.072. https://doi.org/10.1016/j.snb.2015.01.072.
[6] L. Wang, C. Chin, Determination of sulfur in cosmetic products using ion-selective electrode 1, J. Anal. Chem. 62 (7) (2007) 688–690, https://doi.org/10.1134/S1061934807070143.
[7] S. Li, A. Simonian, B.A. Chin, Sensors for agriculture and the food industry, Electrochem. Soc. Interface (2010) 41–46.
[8] M.R. Awual, M. Ismael, T. Yaita, Efficient detection and extraction of cobalt(II) from lithium ion batteries and wastewater by novel composite adsorbent, Sens, Actuators B 191 (2014) 9–18, https://doi.org/10.1016/j.snb.2013.09.076. https://doi.org/10.1016/j.snb.2013.09.076.
[9] L. Rieger, H. Siegrist, S. Winkler, E. Saracevic, R. Votava, J. Nadler, In-situ measurement of ammonium and nitrate in the activated sludge process, Wat. Sci.Tech 45 (4–5) (2002) 93–100.
[10] H. Hirata, Copper(I) sulphide-impregnated silicone rabber membranes as selective electrodes for copper(II) ions, Talanta 17 (1970) 2–6.
[11] R.W. Cattrall, H. Freiser, R.W. Cattrall, Coated wire ion selective electrodes, Anal. Chem. 43 (13) (1971) 1905–1906, https://doi.org/10.1021/ac60307a032.
[12] E. Lindner, R.E. Gyurcsányi, Quality control criteria for solid-contact, solvent polymeric membrane ion-selective electrodes, J. Solid State Electrochem. 13 (2009) 51–68, https://doi.org/10.1007/s10008-008-0608-1.
[13] A. Michalska, All-solid-state ion selective and all-solid-state reference electrodes, Electroanalysis 24 (6) (2012) 1253–1265, https://doi.org/10.1002/elan.201200059.
[14] T. Yin, W. Qin, Trends in analytical chemistry applications of nanomaterials in potentiometric sensors, Trends Anal. Chem. 51 (2013) 79–86, https://doi.org/10.1016/j.trac.2013.06.009. https://doi.org/10.1016/j.trac.2013.06.009.
[15] J. Bobacka, A. Ivaska, A. Lewenstam, Potentiometric ion sensors, Chem. Rev. 108 (2) (2008) 329–351, https://doi.org/10.1021/cr068100w.
[16] S. Wang, Y. Wu, Y. Gu, T. Li, H. Luo, L.H. Li, Y. Bai, L. Li, L. Liu, Y. Cao, H. Ding, T. Zhang, Wearable sweatband sensor platform based on gold nanodendrite array as efficient solid contact of ion-selective electrode, Anal. Chem. 89 (19) (2017) 10224–10231, https://doi.org/10.1021/acs.analchem.7b01560.
[17] M. Fibbioli, W.E. Morf, M. Badertscher, N.F.D. Rooij, È. Pretsch, potential drifts of solid-contacted ion-selective electrodes due to zero-current ion fluxes through the sensor membrane, Electroanalysis 12 (16) (2000) 1286–1292.
[18] G.A. Crespo, S. Macho, F.X. Rius, Ion-selective electrodes using carbon

nanotubes as ion-to-electron transducers, Anal. Chem. 80 (4) (2008) 1316–1322, https://doi.org/10.1021/ac071156l.
[19] E.J. Parra, F.X. Rius, P. Blondeau, A potassium sensor based on non-covalent functionalization of multi-walled carbon nanotubes, Analyst (Cambridge, U.K.) 138 (9) (2013) 2698, https://doi.org/10.1039/c3an00313b. http://xlink.rsc.org/?DOI=c3an00313b.
[20] S. Roy, M. David-Pur, Y. Hanein, Carbon nanotube-based ion selective sensors for wearable applications, ACS Appl. Mater. Interfaces 9 (40) (2017) 35169–35177, https://doi.org/10.1021/acsami.7b07346.
[21] R. Liang, T. Yin, W. Qin, A simple approach for fabricating solid-contact ion-selective electrodes using nanomaterials as transducers, Anal. Chim. Acta 853 (1) (2015) 291–296, https://doi.org/10.1016/j.aca.2014.10.033. https://doi.org/10.1016/j.aca.2014.10.033.
[22] J. Li, T. Yin, W. Qin, An all-solid-state polymeric membrane Pb-selective electrode with bimodal pore C as solid contact, Anal. Chim. Acta 876 (2015) 49–54, https://doi.org/10.1016/j.aca.2015.03.038.
[23] M. Fouskaki, N. Chaniotakis, Fullerene-based electrochemical buffer layer for ion-selective electrodes, Analyst (Cambridge, U.K.) 133 (2008) 1072–1075, https://doi.org/10.1039/b719759d. http://pubs.rsc.org/en/content/articlehtml/2008/an/b719759d.
[24] T. Zhang, C.Z. Lai, M.A. Fierke, A. Stein, P. Bühlmann, Advantages and limitations of reference electrodes with an ionic liquid junction and three-dimensionally ordered macroporous carbon as solid contact, Anal. Chem. 84 (18) (2012) 7771–7778, https://doi.org/10.1021/ac3011507.
[25] C.Z. Lai, M.A. Fierke, A. Stein, P. Bühlmann, Ion-selective electrodes with three-dimensionally ordered macroporous carbon as the solid contact, Anal. Chem. 79 (12) (2007) 4621–4626, https://doi.org/10.1021/ac070132b.
[26] J. Ye, F. Li, S. Gan, Y. Jiang, Q. An, Q. Zhang, L. Niu, Using sp2-C dominant porous carbon sub-micrometer spheres as solid transducers in ion-selective electrodes, Electrochem. Commun. 50 (2015) 60–63, https://doi.org/10.1016/j.elecom.2014.10.014. https://doi.org/10.1016/j.elecom.2014.10.014.
[27] F. Li, J. Ye, M. Zhou, S. Gan, Q. Zhang, D. Han, L. Niu, All-solid-state potassium-selective electrode using graphene as the solid contact, Analyst (Cambridge, U.K.) 137 (3) (2012) 618–623, https://doi.org/10.1039/C1AN15705A. http://xlink.rsc.org/?DOI=C1AN15705A.
[28] R. Hernández, J. Riu, J. Bobacka, C. Vallés, P. Jiménez, A.M. Benito, W.K. Maser, F.X. Rius, Reduced graphene oxide films as solid transducers in potentiometric all-solid-state ion-selective electrodes, J. Phys. Chem. C 116 (42) (2012) 22570–22578, https://doi.org/10.1021/jp306234u.
[29] J. Ping, Y. Wang, J. Wu, Y. Ying, Electrochemistry Communications Development of an all-solid-state potassium ion-selective electrode using graphene as the solid-contact transducer, Electrochem. Commun. 13 (12) (2011) 1529–1532, https://doi.org/10.1016/j.elecom.2011.10.018. https://doi.org/10.1016/j.elecom.2011.10.018.
[30] J. Ping, Y. Wang, Y. Ying, J. Wu, Application of electrochemically reduced graphene oxide on screen-printed ion-selective electrode, Anal. Chem. 84 (7) (2012) 3473–3479, https://doi.org/10.1021/ac203480z.
[31] Z.A. Boeva, T. Lindfors, Few-layer graphene and polyaniline composite as ion-to-electron transducer in silicone rubber solid-contact ion-selective electrodes, Sens, Actuators B 224 (2015) 624–631, https://doi.org/10.1016/j.snb.2015.10.054.
[32] B. Paczosa-Bator, L. Cabaj, M. Pięk, R. Piech, W.W. Kubiak, Carbon-supported platinum nanoparticle solid-state ion selective electrodes for the determination of potassium, Anal. Lett. 48 (17) (2015) 2773–2785, https://doi.org/10.1080/00032719.2015.1045594. https://doi.org/10.1080/00032719.2015.1045594.
[33] B. Paczosa-Bator, L. Cabaj, R. Piech, K. Skupień, Potentiometric sensors with carbon black supporting platinum nanoparticles, Anal. Chem. 85 (21) (2013) 10255–10261, https://doi.org/10.1021/ac402885y.
[34] I. Taurino, G. Sanzó, F. Mazzei, G. Favero, G. De Micheli, S. Carrara, Fast synthesis of platinum nanopetals and nanospheres for highly-sensitive non-enzymatic detection of glucose and selective sensing of ions, Sci. Rep. 5 (October) (2015) 15277, https://doi.org/10.1038/srep15277. http://www.nature.com/articles/srep15277.
[35] J. Xu, F. Jia, F. Li, Q. An, S. Gan, Q. Zhang, A. Ivaska, L. Niu, Simple, Efficient Synthesis, Of gold nanoclusters and their performance as solid contact of ion selective electrode, Electrochim. Acta 222 (2016) 1007–1012, https://doi.org/10.1016/j.electacta.2016.11.069. https://doi.org/10.1016/j.electacta.2016.11.069.
[36] T. Yin, D. Pan, W. Qin, All-solid-state polymeric membrane ion-selective miniaturized electrodes based on a nanoporous gold film as solid contact, Anal. Chem. 86 (22) (2014) 11038–11044, https://doi.org/10.1021/ac5029209.
[37] E. Jaworska, M. Wójcik, A. Kisiel, J. Mieczkowski, A. Michalska, Gold nanoparticles solid contact for ion-selective electrodes of highly stable potential readings, Talanta 85 (4) (2011) 1986–1989, https://doi.org/10.1016/j.talanta.2011.07.049. https://doi.org/10.1016/j.talanta.2011.07.049.
[38] G. Matzeu, C. Zuliani, D. Diamond, Solid-contact ion-selective electrodes (ISEs) based on ligand functionalised gold nanoparticles, electrochim, Acta 159 (2015) 158–165, https://doi.org/10.1016/j.electacta.2015.01.143. https://doi.org/10.1016/j.electacta.2015.01.143.
[39] X. Zeng, W. Qin, A solid-contact potassium-selective electrode with MoO 2 microspheres as ion-to-electron transducer, Anal. Chim. Acta 982 (2017) 72–77, https://doi.org/10.1016/j.aca.2017.05.032. http://linkinghub.elsevier.com/retrieve/pii/S0003267017306992.
[40] F.X. Rius-Ruiz, G.A. Crespo, D. Bejarano-Nosas, P. Blondeau, J. Riu, F.X. Rius, Potentiometric strip cell based on carbon nanotubes as transducer layer: toward low-cost decentralized measurements, Anal. Chem. 83 (22) (2011) 8810–8815, https://doi.org/10.1021/ac202070r.
[41] M. Zhou, S. Gan, B. Cai, F. Li, W. Ma, D. Han, L. Niu, Effective solid contact for ion-selective electrodes: tetrakis(4- chlorophenyl)borate (TB -) anions doped nanocluster films, Anal. Chem. 84 (7) (2012) 3480–3483, https://doi.org/10.1021/ac300473a.
[42] C. Gabrielli, P. Hèlmery, P. Liatsi, M. Masure, H. Perrot, An electrogravimetric study of an all-solid-state potassium selective electrode with prussian blue as the electroactive solid internal contact, J. Electrochem. Soc. 152 (12) (2005), https://doi.org/10.1149/1.2104047. H219.
[43] J. Ping, Y. Wang, K. Fan, W. Tang, J. Wu, Y. Ying, High-performance flexible potentiometric sensing devices using free-standing graphene paper, J. Mater. Chem. B 1 (37) (2013) 4781, https://doi.org/10.1039/c3tb20664e. http://xlink.rsc.org/?DOI=c3tb20664e.
[44] S.T. Mensah, Y. Gonzalez, P. Calvo-Marzal, K.Y. Chumbimuni-Torres, Nanomolar detection limits of Cd2+, Ag+, and K + using paper-strip ion-selective electrodes, Anal. Chem. 86 (15) (2014) 7269–7273, https://doi.org/10.1021/ac501470p.
[45] W. Gao, S. Emaminejad, H.Y.Y. Nyein, S. Challa, Fully integrated wearable sensor arrays for multiplexed in situ perspiration analysis, Nature 529 (7587) (2016) 509–514, https://doi.org/10.1007/128 arXiv:15334406.
[46] T. Guinovart, M. Parrilla, G.A. Crespo, F.X. Rius, F.J. Andrade, Potentiometric sensors using cotton yarns, carbon nanotubes and polymeric membranes, Analyst (Cambridge, U.K.) 138 (18) (2013) 5208, https://doi.org/10.1039/c3an00710c. http://xlink.rsc.org/?DOI=c3an00710c.
[47] J. Hu, A. Stein, P. Bühlmann, A disposable planar paper-based potentiometric ion-sensing platform, Angew. Chem. Int. 55 (26) (2016) 7544–7547, https://doi.org/10.1002/anie.201603017.
[48] M. Novell, M. Parrilla, G.A. Crespo, F.X. Rius, F.J. Andrade, Paper-based ion-selective potentiometric sensors, Anal. Chem. 84 (11) (2012) 4695–4702, https://doi.org/10.1021/ac202979j.
[49] D.P. Rose, M.E. Ratterman, D.K. Griffin, L. Hou, N. Kelley-Loughnane, R.R. Naik, J.A. Hagen, I. Papautsky, J.C. Heikenfeld, Adhesive RFID sensor patch for monitoring of sweat electrolytes, IEEE Trans. Biomed. Eng. 62 (6) (2015) 1457–1465, https://doi.org/10.1109/TBME.2014.2369991.
[50] B. Schazmann, D. Morris, C. Slater, S. Beirne, C. Fay, R. Reuveny, N. Moyna, D. Diamond, A wearable electrochemical sensor for the real-time measurement of sweat sodium concentration, Anal.Meth. 2 (4) (2010) 342, https://doi.org/10.1039/b9ay00184k. http://xlink.rsc.org/?DOI=b9ay00184k.
[51] J. Heikenfeld, Let them see you sweat, IEEE Spectr 51 (11) (2014) 46–63, https://doi.org/10.1109/MSPEC.2014.6934933.
[52] S. Anastasova-Ivanova, B. Crewther, P. Bembnowicz, V. Curto, H.M. Ip, B. Rosa, G.Z. Yang, A wearable multisensing patch for continuous sweat monitoring, Biosens. Bioelectron 93 (2017) 730, https://doi.org/10.1016/j.bios.2017.03.018. https://doi.org/10.1016/j.bios.2016.09.038.
[53] V.A.T. Dam, M.A.G. Zevenbergen, R. Van Schaijk, Flexible chloride sensor for sweat analysis, Procedia Eng 120 (2015) 237–240, https://doi.org/10.1016/j.proeng.2015.08.588. https://doi.org/10.1016/j.proeng.2015.08.588.
[54] S.S. Hassan, S.A. Marei, I.H. Badr, H.A. Arida, Novel solid-state ammonium ion potentiometric sensor based on zirconium titanium phosphate ion exchanger, Anal. Chim. Acta 427 (1) (2001) 21–28, https://doi.org/10.1016/S0003-2670(00)01189-2.
[55] D.O.P. Quan, C.H.U.X. Quang, L.E.T.H.E. Duan, P.H. Viet, A conductive polypyrrole based ammonium ion selective electrode, Environ. Monit. Assess. 70 (2001) 153–165.
[56] A.V. Legin, D.O. Kirsanov, Y.G. Vlasov, Solid-contact polymer sensors based on composite materials, Russ. J. Appl. Chem. 75 (6) (2002) 926–930.
[57] M. Guzinski, J.M. Jarvis, B.D. Pendley, E. Lindner, Equilibration time of solid contact ion-selective electrodes, Anal. Chem. 87 (2015) 6654–6659, https://doi.org/10.1021/acs.analchem.5b00775.
[58] A. Michalska, A. Hulanicki, All solid-state hydrogen ion-selective electrode based on a conducting poly(pyrrole) solid contact, Analyst (Cambridge, U.K.) 119 (1994) 2417–2420.
[59] J. Zhang, Y. Guo, S. Li, H. Xu, A solid-contact pH-selective electrode based on tridodecylamine as hydrogen neutral ionophore, Meas. Sci. Technol. 27 (2016) 105101, https://doi.org/10.1088/0957-0233/27/10/105101.
[60] R.W. Licht, Lithium : still a major option in the management of bipolar disorder acute antimanic actions of lithium, CNS neurosci, Therapy 18 (2012) 219–226, https://doi.org/10.1111/j.1755-5949.2011.00260.x.
[61] K.A. Kaplan, A.G. Harvey, Behavioral treatment of insomnia in bipolar disorder, Am. J. Psychiatr. 170 (7) (2013) 716–720, https://doi.org/10.1176/appi.ajp.2013.12050708.Behavioral.
[62] V. Umamaheswari, A. Avasthi, G.S. Risk, Risk factors for suicidal ideations in patients with bipolar disorder, Bipolar Disord 16 (2014) 642–651, https://doi.org/10.1111/bdi.12179.
[63] M. Pompili, M. Innamorati, M. Raja, G. Ducci, G. Angeletti, D. Lester, P. Girardi, R. Tatarelli, E.D. Pisa, Suicide risk in depression and bipolar disorder : do impulsiveness-aggressiveness and pharmacotherapy predict suicidal intent ? Neuropsychiatric Dis. Treat. 4 (1) (2008) 247–255.
[64] A. Muneer, Staging models in bipolar disorder : a systematic review of the literature, clin. Psychopharmacol, Neuroscience 14 (2) (2016) 117–130.
[65] D. Gruson, A. Lallali, A.M. Taburet, A. Legrand, M. Conti, L.D. Biochimie, Evaluation of a new lithium colorimetric assay performed on the Dade Behring

Dimension X-pand system, Clin. Chem. Lab. Med. 42 (9) (2004) 1066–1068, https://doi.org/10.1515/CCLM.2004.214.
[66] H.S. Hopkins, J. Gelenberg, Serum lithium levels and the outcome of maintenance therapy of bipolar disorder, Bipolar Disord 2 (2000) 174–179.
[67] G.D. Christian, Reagents for lithium electrodes and sensors for blood serum, Sensors 2 (2002) 432–435.
[68] B. Rumbelow, M. Peake, Performance of a novel spectrophotometric lithium assay on a routine biochemistry analyser, Ann. Clin. Biochem. 38 (2001) 684–686.
[69] R.H. Christenson, J.J. Mandichak, S. Hong, J.M. Augustyn, J.C. Thompson, Clinical performance characteristics of a new photometric lithium assay : a multicenter study, Clin. Chim. Acta 327 (2003) 157–164.
[70] W. Glazer, J. Sonnenberg, M. Reinstein, R. Akers, A novel, point-of-care test for lithium levels: description and Reliability, J. Clin. Psychiatry 65 (5) (2004) 652–655.
[71] M. Novell, T. Guinovart, P. Blondeau, F.X. Rius, F.J. Andrade, A paper-based potentiometric cell for decentralized monitoring of Li levels in whole blood, Lab a Chip 14 (7) (2014) 1308, https://doi.org/10.1039/c3lc51098k. http://xlink.rsc.org/?DOI=c3lc51098k.
[72] F. Coldur, M. Andac, All-solid-state polyvinyl chloride membrane lithium-selective electrode with improved selectivity and its application in serum lithium assay, Sens. Lett. 9 (5) (2011) 1738–1744, https://doi.org/10.1166/sl.2011.1717. URL http://openurl.ingenta.com/content/xref?genre=article{\&}issn=1546-198X{\&}volume=9{\&}issue=5{\&}spage=1738.
[73] F. Coldur, M. Andac, A flow-injection potentiometric system for selective and sensitive determination of serum lithium level, Electroanalysis 25 (3) (2013) 732–740, https://doi.org/10.1002/elan.201200466.
[74] M. Kamenica, R.R. Kothur, A. Willows, B.A. Patel, Lithium ion sensors, Sensors 17 (2017) 2430, https://doi.org/10.3390/s17102430.
[75] G. Sanzó, I. Taurino, R. Antiochia, L. Gorton, G. Favero, F. Mazzei, G.D. Micheli, S. Carrara, Bioelectrochemistry Bubble electrodeposition of gold porous nanocorals for the enzymatic and non-enzymatic detection of glucose, Bioelectrochemistry 112 (2016) 125–131, https://doi.org/10.1016/j.bioelechem.2016.02.012. https://doi.org/10.1016/j.bioelechem.2016.02.012.
[76] J. Bobacka, Potential stability of all-solid-state ion-selective electrodes using conducting polymers as ion-to-electron transducers, Anal. Chem. 71 (21) (1999) 4932–4937, https://doi.org/10.1021/ac990497z.
[77] E. Lindner, Y. Umezawa, Performance evaluation criteria for preparation and measurement of macro- and microfabricated ion-selective electrodes (IUPAC Technical Report), Pure Appl. Chem. 80 (1) (2008) 85–104, https://doi.org/10.1351/pac200880010085.
[78] E. Bakker, Selectivity of liquid membrane ion-selective electrodes, Electroanalysis 9 (1) (1997) 7–12, https://doi.org/10.1002/elan.1140090103.
[79] F. Coldur, M. Andac, I. Isildak, Flow-injection potentiometric applications of solid state Li + selective electrode in biological and pharmaceutical samples, J. Solid State Electrochem. 14 (12) (2010) 2241–2249, https://doi.org/10.1007/s10008-010-1070-4.
[80] K. Kimura, H. Yano, S. Kitazawa, T. Shono, Synthesis and selectivity for lithium of lipophilic 14-crown-4 derivatives bearing bulky substituents or an additional binding site in the side arm, J. Chem. Soc. Perkin Trans. I (1986) 1945–1951, https://doi.org/10.1039/P29860001945.